European Polymer Journal 216 (2024) 113308

Contents lists available at ScienceDirect

European Polymer Journal

journal homepage: www.elsevier.com/locate/europolj

Production of polycaprolactone foams incorporating *Hibiscus sabdariffa* extract

Paolo Trucillo [a,b,*], Viviana Nebbioso [a], Pier Francesco Ferrari [c,d,e], Daniele Naviglio [f], Ernesto Di Maio [a,b]

[a] *Dipartimento di Ingegneria Chimica, dei Materiali e della Produzione Industriale, University of Naples Federico II, P.le V. Tecchio, 80 80125, Napoli, Italy*
[b] *Foamlab, University of Naples Federico II, P.le V. Tecchio, 80 I-80125, Napoli, Italy*
[c] *Department of Civil, Chemical and Environmental Engineering, University of Genoa, via Opera Pia, 15 16145, Genoa, Italy*
[d] *Research Center for Biologically Inspired Engineering in Vascular Medicine and Longevity, University of Genoa, via Montallegro, 1 16145, Genoa, Italy*
[e] *IRCCS Ospedale Policlinico San Martino, largo Rosanna Benzi, 10 16132, Genoa, Italy*
[f] *Dipartimento di Scienze Chimiche, University of Naples Federico II, via Cintia, 4 80126, Naples, Italy*

ARTICLE INFO

Keywords:
Foams
Karkadé
Drug release
Biomaterials
Human keratinocytes

ABSTRACT

Hibiscus sabdariffa is a plant characterized by a high content of antioxidant molecules; its aqueous extract (*karkadé*) offers considerable potential benefits during the healing process. Since most antioxidant molecules are sensitive to thermo-oxidative degradation during extraction and encapsulation processes, this study proposes a novel application to preserve *karkadé* inhibition power, by entrapping it in poly-ε-caprolactone (PCL) foams. *Karkadé* was obtained using Rapid Solid-Liquid Dynamic Extraction, processed at 20 °C and below 10 bar. The concentration of *karkadé* solid residue was 195.0 ± 4.6 g/L, while the reduction of the antioxidant inhibition power was 26.0 ± 1.4 % after 450 min of extraction, much greater than native *karkadé* extracted using other techniques (>60 %). Entrapment of *karkadé* occurred during the preparation of 3 mg/mL PCL in an acetone solution, which solidified upon solvent evaporation at 20 °C, obtaining a disk. Then, the disk was foamed using CO_2 as physical blowing agent at optimized parameters (45 °C, 100 bar, and sorption for 60 min). Foam density of 180 kg/m^3, cell number density of 4.1E06 cell/cm^3, and an average pore dimension of 56 ± 28 μm were obtained, with k*arkadé* entrapment efficiency up to 97 %. This study focused on manipulating PCL foam cells density and diameter, to influence release time of *karkadé* extract into an aqueous receiving medium. Different cells diameters and number density were achieved by varying sorption time of CO_2 in PCL, set at 30, 60, and 90 min, respectively. Sorption time of 60 min was demonstrated to be sufficient for creating a uniform porous structure, while a 30 min sorption time resulted in a delayed release rate. Foams were soaked in cell culture medium, which was then put in contact with human keratinocytes, thus demonstrating their biocompatibility up to 9 days.

1. Introduction

The plant *Hibiscus sabdariffa*, a member of the *Malvaceae* family, stands as a botanical specimen of considerable interest [1]. Indigenous to tropical Africa [2–4], this plant obtained much attention for the multifaceted attributes and applications of its aqueous extract whose commercial name is *karkadé* [5] Having dark green leaves with serrated margins, its crimson-hued fleshy calyces are particularly rich in bioactive compounds. Recognized for its antioxidant properties, *H. sabdariffa* has been extensively used in cosmetic formulations, with demonstrated effects on hair strength and growth stimulation. Nowadays, *H. sabdariffa* continues capturing attention also for the anti-aging properties of its extract [6–9]. The numerous molecules contained in karkadé are known for their significant antioxidant properties [10,11], but their preservation is particularly challenging, due to the rapid thermal degradation they undergo using maceration or percolation

Abbreviations: **DSs**, Delivery Systems; **PCL**, Poly-ε-caprolactone; **BA**, Blowing Agent; **ER**, Expansion Ratio; **EE**, Encapsulation Efficiency; **RSLDE**, Rapid Solid-Liquid Dynamic Extraction; **AA**, Antioxidant Activity; **SEM**, scanning electron microscopy; **CM**, Conditioned Media; **DMEM**, Dulbecco's modified Eagle's medium.

* Corresponding author.
E-mail addresses: paolo.trucillo@unina.it (P. Trucillo), viviana.nebbioso@unina.it (V. Nebbioso), pier.francesco.ferrari@unige.it (P.F. Ferrari), naviglio@unina.it (D. Naviglio), edimaio@unina.it (E. Di Maio).

https://doi.org/10.1016/j.eurpolymj.2024.113308
Received 29 April 2024; Received in revised form 12 July 2024; Accepted 12 July 2024
Available online 14 July 2024
0014-3057/© 2024 The Author(s). Published by Elsevier Ltd. This is an open access article under the CC BY-NC-ND license (http://creativecommons.org/licenses/by-nc-nd/4.0/).

techniques (inhibition power reduced to a value larger than 60 %) that expose them to temperatures larger than 50 °C. Therefore, as common technique used for different delivery systems (DSs), it is necessary to use an extraction process at lower working temperatures, while designing specific and biocompatible encapsulation devices [12].

The described issue can be addressed through the utilization of polymeric foams loaded with bioactive molecules [13–21]. Characterized by a solid continuous matrix enveloping gaseous phase void, foams represent a versatile solution to this challenge. Among the methods commonly known for their production, gas foaming is particularly noteworthy, finding applications in fields such as packaging, acoustic and thermal insulation, energy absorption, separation processes, and tissue engineering [22–26]. Carbon dioxide is the most employed blowing agent (BA) in gas foaming, since it is not-expensive, non-toxic, non-flammable, and non-explosive [27,28]. Moreover, supercritical carbon dioxide is commonly used for biological applications due to its low critical temperature (31 °C, which prevents compound degradation arising above 50 °C), high diffusivity achieved at relatively low pressures, and its inert behavior with molecules that need to be encapsulated in DSs. Polymeric foams designed as drug DSs were demonstrated to be particularly versatile in nutraceutical and pharmaceutical applications: poly(lactic-*co*-glycolic acid) foams offer a biocompatible device for controlled release kinetics [29–31]; polyurethane foams, designed for flexibility and precision, serve as dynamic carriers for therapeutic agents [32]; chitosan-based foams and foam coatings exhibit biocompatibility and mucoadhesive properties, making them effective for targeted drug release in wound healing and mucosal applications [33,34]. These foam-based DSs provide a controlled and tailored drug release profiles, enhancing bioactives efficacy.

Among polymeric foams used for drug delivery, those based on poly-ε-caprolactone (PCL) are noteworthy [35,36]. PCL is a semicrystalline non-hazardous polymer belonging to the family of polyesters and it is synthesized through the ring-opening polymerization of ε-caprolactone. PCL is characterized by a relatively low cost, minimal supply risk, and easy modification of its biological and mechanical properties through the manipulation of processing operating parameters. PCL has a glass transition temperature of approximately 60 °C and a melting point of about 60 °C [37], thus making it optimal for pharmaceutical and wound healing applications [38,39]. Having a high blend compatibility [40,41], PCL-based formulations are characterized by an overall moderate release rate and extended degradation times in an aqueous environment [42]. In tissue engineering, PCL scaffolds are employed for the replacement of hard tissues, especially when wounds necessitate extended healing times [43–45]. Moreover, PCL is particularly versatile as DS, since it has been proposed in various administration formulations [46–48] such as micro- and nanoparticles for oral, intravenous, and pulmonary delivery. However, PCL-based formulations often exhibit two drawbacks: an initial drug burst release occurring soon after administration and high hydrophobicity, with lack of selectivity to target tissues and unwanted drug accumulation in healthy sites, resulting in potential side effects.

PCL-based foams [49] engineered for topical delivery offer a versatile platform with diverse applications [50], ensuring controlled release of therapeutic agents for optimized healing. Dermatological formulations, such as those for acne or eczema, utilize PCL foams to provide targeted treatment with enhanced adherence. Additionally, PCL-based foams are employed in transdermal drug DSs, allowing controlled release through the skin for both dermatological and systemic applications, thus highlighting efficacy of PCL-based foams in advancing topical delivery strategies. Indeed, patches could offer a solution for skin penetration administration, assuring direct contact with the target tissue and providing tunable drug release and absorption [51–54].

In this study, *karkadé* was obtained from *H. sabdariffa* using Rapid Solid-Liquid Dynamic Extraction (RSLDE), which operates at mild pressure and room temperature conditions [55]. Subsequently, the aqueous extract was entrapped into polymeric foams, with the aim of designing a patch-prototype for controlled *karkadé* release. PCL devices were prepared by optimizing physical foaming parameters of PCL disks [56]. Rigidity, pore size, pore numerical density, molecular weight, shape, and thickness were optimized, as well as temperature and pressure conditions. Another objective of this work was to obtain a lightweight material for topical delivery, while providing an efficient and controlled release mechanism though the variation of polymer-to-drug ratio, that often affects release in terms of kinetic and delaying effects. Scanning electron microscope analysis was also performed, establishing a correlation between *karkadé* release time and pores number density and dimensions. Tests with human keratinocytes completed the study to demonstrate PCL foams biocompatibility.

2. Materials

Hibiscus sabdariffa flowers have been purchased from Blanks GmbH & Co. KG, Uplengen, Germany, and were used in the extraction process in the same form as they were received. Poly-ε-caprolactone (PCL) (CAS Number 24980–41-4) has been purchased from Perstorp AB, Malmö (Sweden), with the brand name CAPA® 6501 and has been used as received. Its main properties are summarized in Table 1.

The extractant main component was tap water, while citric acid (CAS number 77–92-9) and potassium sorbate (CAS number 24634–61-5) were purchased from Alfasigma, Bologna, Italy. These components were mixed to prepare the aqueous phase used as extracting solvent in RSLDE process. Acetone (CAS number 67–64-1) and 2,2-diphenyl-1-picrylhydrazyl (CAS number1898-66–4) have been purchased from Sigma-Aldrich, Milan, Italy. Carbon dioxide (CAS number 99.8 124–38-9) was purchased from Sol S.p.A., Monza, Italy. Dulbecco's modified Eagle's medium, fetal bovine serum, penicillin/streptomycin for cell culture, and phosphate buffered saline were bought from Carlo Erba, Milan, Italy.

3. Methods

3.1. Extraction process

Karkadé has been obtained using RLSDE technique. This process has been developed following the evolution of the double syringe method [57]. According to this principle, the solvent was forced to overcome the leaf barrier, thus creating a pressure gradient between the inside and the outside of natural matter [58]. A sketch of the process is reported in Fig. 1. In details, 100 g of *H. sabdariffa* flowers (indicated as "6″ in Fig. 1) were added to a food-grade polyethylene bag inserted in the extractor (indicated as "5" in Fig. 1) and then processes in 500 mL of tap water containing 0.15 % (w/w) citric acid and 0.2 % (w/w) potassium sorbate. Once closed the extractor, the liquid filled inside was compressed and forced to overcome the natural external barrier of leaves, thus solubilizing the internal molecules. This step is called "compression step" (indicated as "3" in Fig. 1). Once reached the pressure of about 10 bar (measured by a manometer mod. MSS208010, Comhas S.r.L., Cinisello Balsamo, Italy, indicated as "7" in the sketch), the static phase took place, apparently stopping the process for a defined amount of time.

Table 1
Properties of PCL (data provided by the manufacturer).

Property	Value
average molecular weight	80,000 g/mol
supplied form	pellet
pellet diameter	3 mm
crystalline fraction	60–70 %
density	1145 kg/m^3
T_g	−60 °C
T_m	60 °C at 1 bar
water content	< 1 %
elongation at break	800 %

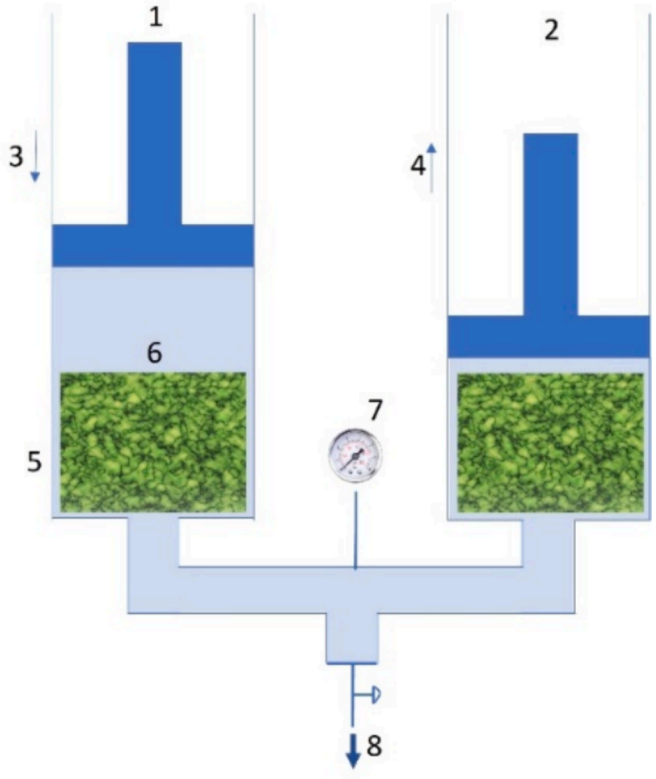

Fig. 1. A sketch of the RLSDE process. (1) and (2) represent a schematization of the two syringes forcing the liquid inside the reactor (5). Leaves and other natural matter are described in (6), while (7) is the manometer and (8) the withdrawal valve of the liquid. (3) represents the compression phase while (4) the release phase.

Then, the syringes/pistons (indicated as "1" and "2" in Fig. 1) were released and the liquid containing the extracted molecules diffused back to the external liquid bulk. This second phase is called dynamic and has the same duration of compression phase (reported as "4" in Fig. 1). In this process, a cycle of extraction had a duration of four minutes while static phase and dynamic phase had 2 min duration each. At the end, the solutes-enriched liquid was discharged by the extractor (indicated as "8" in Fig. 1) and withdrawn by the operator. To determine the extraction yield and antioxidant activity (AA) of *karkadé*, RLSDE process was stopped at different time intervals (from 36 min to about 450 min) and the aqueous extract was analyzed at each time as follows: 10 mL extract were withdrawn after stopping the experiment, dried in a stove at 105 °C and then the solid residue was weighted.

3.2. Preparation of foam precursors

As indicated in the section 3.1, the aqueous nature of *karkadé* makes it impossible to directly dissolve PCL beads to create a unique mixture. For this reason, *karkadé* has been previously entrapped in a PCL solid precursor, whose preparation is described as follows. The chosen shape for the precursor was a disk with a diameter of 25 and a height of 8 mm. To prepare these disks, a glass vial (diameter of 27 and height of 70 mm) has been used (Fig. 2a). In details, 3 g of PCL beads were dissolved in 3 mL acetone; the solution was heated at 80 °C until reaching dissolution. Then, the solution was slowly cooled to 35 °C; at that temperature, a defined amount of *karkadé* was added to the solution using a pipet (Fig. 2b), while being still liquid. Following diffusion in the molten polymeric matrix, we assumed that the distribution of *karkadé* during cooling of the disk was uniform. Once the liquid has been injected, the solution has been dried under vacuum for 120 min and then left drying at room conditions for 24 h until solidification. The final solid disk had a smooth surface and regular shape (Fig. 2c). Then, PCL disks were foamed in a cubic aluminum mould, obtaining a cubic shape (Fig. 2d).

3.3. Foaming process

As shown in the sketch of Fig. 3, high-pressure autoclave (indicated as "5″ in Fig. 3) was equipped with a heating system (indicated as "7" in Fig. 3) and sensors for the control of temperature and pressure (indicated as "1" in Fig. 3). The experiments were performed by injecting CO_2 under sub-critical or supercritical conditions within the autoclave. The autoclave was pressurized using a CO_2 pump (indicated as "4" in Fig. 3) (model Nex10, Supercritical Fluid Technologies Inc., Newark, United States). In details, this apparatus is characterized by a stainless-steel reactor (0.3 L internal volume, model BC-1, HiP, Erie, USA), an electrical heater controlled through a PID PLC (Gefran 1850), and a pressure transducer (model P943, H. G. Schaevitz LLC, Alliance Sensors Group, Pennsauken, NJ, USA). Pressure and temperature data were collected using a data acquisition system (Gefran GF_eXpress), as optimized systems in comparison to similar works [59,60]. The accuracy for the measurements of the pressure was 0.1 bar and 0.1 °C for temperature, respectively. The pressure release was activated by a discharge ball

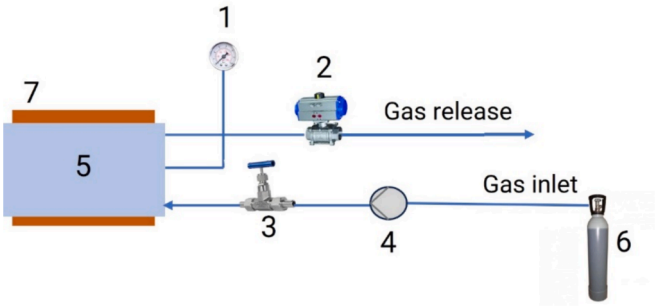

Fig. 3. A sketch of the foaming process: 1. Pressure gauge; 2. Electrovalve; 3. Needle valve; 4. Pump; 5. Reactor; 6. Carbon dioxide storage; 7. Reactor heating system.

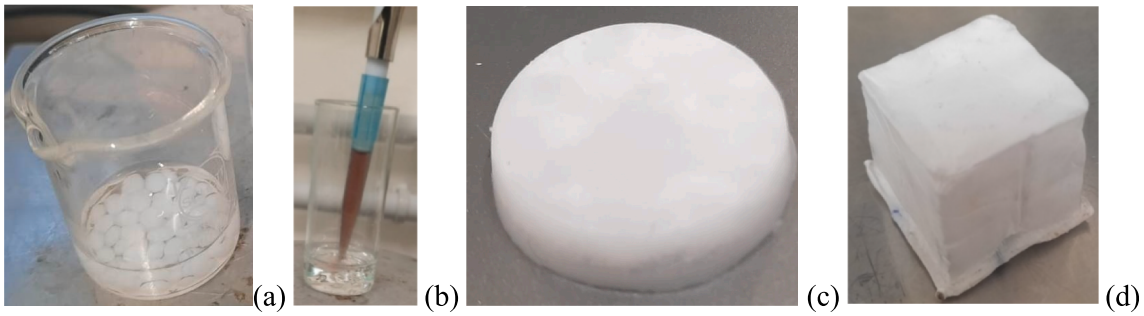

Fig. 2. Images of pellets in acetone solution (a), karkadé addition to PCL in acetone solution (b), dried solid disk (c), foamed sample (d).

valve (model 15–71 NFB, HiP, Erie, USA), an electromechanical actuator (model 15–72 NFB TSR8, HiP, Erie, USA), and an electrovalve (indicated as "2" in Fig. 3).

In details, the polymeric PCL disk was inserted in an aluminum cubic mould and processed through physical foaming. This process consists in first melting the polymer up to a specific fusion peak temperature; then, a BA diffuses through the polymer, solubilizing it from the external surfaces to the center. After reaching saturation, gas is suddenly released, thus involving nucleation of bubbles, and the consequent formation of cells. Following Fig. 3, the mould was inserted in the reactor and heated to the desired temperature, which was defined for each experiment within the range of 30 to 55 °C. The autoclave was pressurized with the BA until the desired pressure, defined for each experiment within the range of 50 to 150 bar. Filling of CO_2 in the autoclave up to 100 bar was completed in about 6 min; in the final part of the experiment, CO_2 was released from the autoclave, thus causing a sudden pressure reduction down to 1 bar. During pressure release, bubbles nucleation and growth occurred, until stabilization of the foam. Release of CO_2 from the autoclave (from 100 to 1 bar) was completed in 5 ± 1 s.

The main objective of this work consists in the variation of foam cellular density and diameter, thus resulting in different barriers to *karkadé* release time in the receiving medium. To achieve this result, CO_2 in PCL sorption time was set at 30, 60, and 90 min, respectively. Considering that carbon dioxide diffusivity (in the range of this works' operating parameters) is included between 1E and 09 and 1E-08 m^2/s (Ushiki et al. [63]), sorption time of 60 min was estimated to be sufficient to obtain a uniform porous structure. Therefore, another experiment was performed with a sorption time of 30 min to obtain a not uniform structure, while the third experiment performed at 90 min sorption time, was aimed at demonstrating to have a similar structure than the foam produced at 60 min.

4. Samples characterization

The AA, also defined as antioxidant power, was determined using the 2,2-diphenyl-1-picrylhydrazyl (DPPH) assay to measure the scavenging capacity of radicals dissolved in karkadé aqueous extracts. Initially, a 0.005 % (w/w) solution of DPPH in methanol has been prepared. Afterwards, 100 μL of the sample were added to 900 μL of DPPH solution. After waiting 1 h in absence of light, the absorbance was measured using a spectrophotometer (Onda V10 Plus, Giorgio Bormac S.r.L., Milan, Italy) at the wavelength of 517 nm, and the AA was calculated using Eq. (1) and Eq. (2):

$$\textit{Antioxidant activity}\,(AA),\ \% = \frac{A_{CTR} - A_{sample}}{A_{CTR}} * 100 \tag{1}$$

$$\textit{Inibition of the antioxidant activity},\ \% = (100 - \mathrm{AA}) \tag{2}$$

where A_{CTR} is the control reaction absorbance, obtained without sample, while A_{sample} is the specimen absorbance [61]. The inhibition of the antioxidant power/activity was intended as a complement to 100 % of the Eq. (2).

The densities of the foams were calculated at room temperature, as indicated in the Eq. (3):

$$\rho_f = \rho_w \frac{m_1}{m_1 - m_2} \tag{3}$$

where m_1 is the weight of sample measured in air medium, while m_2 is the weight of the same sample submerged in water, being ρ_w water density. The Expansion Ratio (ER) is determined as the ratio of densities before and after the foaming process.

$$\mathrm{ER} = \frac{\rho_{nf}}{\rho_f} \tag{4}$$

where ρ_f is the density of the foamed samples while ρ_{nf} is the density of the not foamed sample, i.e., the solid. Foamed samples were observed using Scanning Electron Microscopy (SEM, mod. Merlin VP compact, Carl Zeiss, Oberkochen, Germany). Cell number density was obtained after analyzing SEM images with Fiji software (National Institutes of Health, Bethesda, MD, USA), indicated as the number of cells nucleated per unit volume of the original unfoamed polymer (N_0), as indicated in Eq. (5), whose specific explanations were reported elsewhere [62].

$$N_0 = \left(\frac{n}{A}\right)^{\frac{3}{2}} \frac{1}{1 - \frac{\rho_f}{\rho_{nf}}} \tag{5}$$

where n represents the number of cells counted in the SEM image, A is the area of the micrograph, as reported in the literature [63].

The Entrapment Efficiency (EE), intended as the amount of *karkadé* retained by the polymer disk after solidification, and the *karkadé* release tests from prepared foams, have been performed using the spectrophotometer reported above. This instrument is equipped with a single laser optical system, power 75 W, absorbance stability of ± 0.002 Abs/h, operating in the visible range 325–1000 nm. To measure the EE of *karkadé*, foams were again dissolved in a known volume of acetone and the *karkadé* absorbance was measured. Having a typical violet color, *karkadé* molecules were identified by a unique absorbance peak at 340 nm, as also confirmed by the literature [64]. The EE was calculated as follows:

$$EE = \frac{C_{entrapped}}{C_{total}} * 100 \tag{6}$$

where the C_{total} represents the *karkadé* concentration in the known initial aqueous volume injected during the preparation of the disk, while $C_{entrapped}$ represents the concentration of *karkadé* dissolved in acetone after foam dissolution. The ratio expressed by Eq. (6) is the general formula used to calculate the EE in drug loaded systems [65–67]; in this case, it is related to the amount of *karkadé* extract that was efficiently retained by the foamed polymer after gas release. To perform these experiments, calibration curves of *karkadè* in acetone and water have been prepared (Figure S1).

Preliminary foams geometry was achieved with a rectangular aluminum mould having a free volume of 40 × 40 × 10 mm^3. Patch-like foamed samples were produced using a different mould geometry. In particular, the mould had dimensions of 95 × 12 × 10 mm^3, with a PCL beads mass of 3 g per experiment. Being the patch prototype made by a single material, the EE was measured in the center and also at the extremities of the sample. Moreover, to assess cell viability, PCL foams underwent a rigorous sterilization process. Initially, they were immersed in a solution of phosphate buffered saline containing penicillin/streptomycin (1 %, v/v) for 15 min under sterile conditions. Subsequently, the foams underwent two additional washing steps, each lasting 8 min, using the same solution. Then, the foams were completely immersed in Dulbecco's modified Eagle's medium (DMEM) enriched with fetal bovine serum (10 %, v/v) and placed in a shaker (Continental Instrument, Milan, Italy) at 7 rpm and stored at 37 ± 2 °C (incubator INCU-Line 250R Premium, VWR International, Radnor, PA, USA) for a total period of 20 h. This facilitated the recovery of various molecules released from the foams, obtaining conditioned media (CM). Throughout the extraction process, a consistent solid/liquid ratio of 1:10 (w/v) was maintained.

Human keratinocytes (HaCaT cells) were used to evaluate potential cytotoxicity of PCL foams. However, to take into consideration the effects of the released molecules and the degradation by-products, the extraction process was conducted without direct contact with the cells for 20 h. Prior to interaction with the CM, HaCaT cells were seeded at a density of 4 × 10^3/well in a 96-well plate containing complete medium. Cell viability was then assessed using the CellTiter96® AQ_{ueous} One Solution Cell Proliferation Assay according to the manufacturer's protocol (Promega, Madison, WI, USA). Briefly, at various time-points (1, 2,

3, 4, 5, and 9 days), 20 μL of the reagent was added to each culture well, and the resulting formazan product, generated by the bioreduction of tetrazolium by cells, was measured spectrophotometrically at 492 nm using a microplate reader (GloMax® Discover, Promega, Madison, WI, USA). All experiments were conducted in triplicate to ensure the accuracy and reliability of the results.

5. Results

5.1. Extraction of karkadé mixture

The initial concentration of flowers in tap water was 200 g/L (i.e., 100 g *H. sabdariffa* in 0.5 L tap water). *Karkadé* extracted using RSLDE technique has been characterized in terms of solid residue and inhibition of the antioxidant power. Experiments and relative measurements were performed in triplicates at regular time intervals during extraction process (see Table 2).

The concentration plateau was easily reached after about 6 h, with a solid residue concentration of 188.4 ± 5.0 g/L. In the following hours, only a slight increase in solid residue concentration was achieved. Due to the low increase of extraction yield and to the significant increase of the antioxidant inhibition power, it was considered not convenient to continue the extraction over 450 min extraction cycles. Indeed, the inhibition of the antioxidant power stabilized on a value of about 15 % until 268 min extraction; however, in the period included among 270 and 450 min, the antioxidant inhibition power was increased from 15 to 26 %, probably due to degradation phenomena. Therefore, in the following experiments, the extract entrapped in foams was withdrawn after at 270 min extraction.

5.2. Foaming

5.2.1. Effect of temperature and pressure

The first foaming experiments were aimed at finding the best conditions of temperature and pressure, to achieve the highest ER. According to results already present in literature [68], the range of temperature values explored in this study was 30–55 °C, lower than PCL melting temperature (60 °C) at 1 bar. The use of processing temperatures lower than melting point is possible, considering the plasticization effect [69] exerted by carbon dioxide in supercritical conditions. In these experiments, the pressure was set at 100 bar; therefore, the plasticizing effect of carbon dioxide reduced melting temperature in the range 20–30 °C, as reported in the literature [70]. Temperature never exceeded 55 °C to avoid thermal degradation of bioactive molecules.

The effect of temperature was studied by setting a sorption time of 90 min, overestimated considering diffusivity [71] values reported for carbon dioxide in PCL [72,73]. The precursor was a 3 g PCL disk, prepared as described in section 3.2. Values of densities were calculated using Eq. (3) and the ER with Eq. (4) (see Section 4).

Considering results reported in Table 3, the effect of temperature significantly modified the rigidity of the materials, as well as the final density. At the end of this temperature range exploration, a minimum density of about 180 kg/m^3 was achieved at the temperature of 45 °C. Therefore, all the following experiments were performed by setting this temperature value.

The effect of pressure was another operating parameter studied in this work. Also in this case, according to the previously reported literature [72,73], a range between 50 and 150 bar was explored, while all the previous conditions were left constant. By working at sub-critical pressure (50 bar), the density of the foam was almost identical to the not foamed PCL (1145 kg/m^3); indeed, in this case, the disk appeared almost unchanged in terms of ER. At these conditions (45 °C and 50 bar), the polymer remained in solid conditions without reaching melting peak. Therefore, sub-critical pressure (50 bar) was not sufficient to operate with PCL beads. At 75 bar, the density of the foam significantly decreased to about 350 kg/m^3, while at 100 bar, density was 180 ± 20 kg/m^3. At the largest pressure explored (150 bar), a quite similar density of about 210 kg/m^3 was obtained, considering measurement errors. Therefore, operating at 100 bar represented the best working condition to minimize the mass of CO_2 and to maximize the expansion ratio of PCL foams.

5.2.2. Production of foams loaded with karkadé

In this section of the work, foams incorporating *karkadé* were designed using a cubic mould geometry. As detailed in the Methods section, a defined amount of aqueous extract was entrapped within PCL disks before cooling and drying, thus defining a specific polymer-to-drug ratio. Subsequently, the disks were subjected to a high-pressure foaming procedure, as described earlier. The objective of these experiments was to maximize the incorporation of *karkadé* in foams while achieving tunable release the inner core to the external aqueous bulk. According to previous experiments performed on unloaded foams, temperature was set at 45 °C, pressure at 100 bar, while sorption time at 30, 60, and 90 min, respectively. The extract mass was also varied from 0.10 to 0.6 g, corresponding to a polymer-to-drug ratio of 30, 10, and 5 g/g, respectively, as reported in Table 4.

As indicated in Table 4, a sorption time of 30 min resulted in the production of a not uniform foamed sample, thus having an average density of about 350 kg/m^3; instead, 60 min corresponded to a sufficient

Table 2
Extractive yield and AA monitored over time during RLSDE.

Extraction time, min	Solid residue, g/L	Inhibition of antioxidant power/activity, %
0	0	0
36	21.6 ± 2.5	15.8 ± 1.5
72	43.6 ± 3.1	14.8 ± 2.0
112	75.1 ± 2.9	15.5 ± 1.7
148	105.8 ± 3.5	15.1 ± 2.5
208	132.2 ± 2.4	14.5 ± 3.4
268	157.4 ± 2.7	15.1 ± 3.0
328	177.5 ± 3.8	19.5 ± 1.7
358	188.4 ± 5.0	20.0 ± 2.0
388	193.1 ± 4.5	21.5 ± 2.1
418	195.0 ± 4.9	25.1 ± 1.9
448	195.0 ± 4.6	26.0 ± 1.4

Table 3
Density and ER of unloaded foams produced at 90 min sorption time.

Temperature, °C	Pressure, bar	Foam density, kg/m^3	ER, %
30	100	260 ± 30	440 ± 103
40	100	270 ± 20	424 ± 63
42	100	290 ± 30	395 ± 83
45	50	1150 ± 20	100 ± 3
45	75	350 ± 30	327 ± 56
45	100	180 ± 20	636 ± 143
45	150	210 ± 20	545 ± 105
48	100	560 ± 30	204 ± 22
55	100	500 ± 40	229 ± 37

Table 4
Foams prepared at 100 bar and 45 °C, loaded with *karkadé* at different PCL/extract ratio.

Sorption time, min	Polymer-to-Drug ratio, g/g	Foam density, kg/m^3	EE foam, %
30	30	350 ± 30	91.6 ± 0.9
30	10	360 ± 40	90.5 ± 0.5
30	5	340 ± 50	92.3 ± 0.3
60	30	190 ± 30	97.3 ± 0.8
60	10	200 ± 20	91.5 ± 0.5
60	5	190 ± 30	89.3 ± 0.9
90	30	210 ± 20	90.5 ± 0.5
90	10	220 ± 10	94.4 ± 0.7
90	5	200 ± 20	91.7 ± 0.3

sorption time to obtain a uniform foam, having a density of about 190 kg/m^3. By working with a 30 min excess time (total sorption of 90 min), samples had similar density than the ones produced at 60 min sorption. Compared to unloaded foams, the density of uniform and not uniform samples was not significantly affected by the presence of *karkadé*. Moreover, each sample revealed a negligible *karkadé* loss due to foaming process.

5.2.3. SEM characterization

As indicated in the Methods section, foams were obtained with a gas release rate of about 15 bar/s. Therefore, pressure drop was essential for obtaining highly interconnected porosities. Since the surface of the samples was smooth and characterized by closed cells, the observations and further pores characterization were performed on a section of the sample. The sample analyzed in Fig. 4a and Fig. 4b was processed at 100 bar, 45 °C and 60 min and was not loaded with *karkadé* extract. Instead, while Fig. 4c and Fig. 4d reports a foam produced at the same conditions with 0.30 g *karkadé* loading.

The images in Fig. 4a and Fig. 4b depict a uniform porous structure and are related to a drug-free sample, with an average density of 180 ± 20 kg/m^3 (see the experiment performed at 45 °C and 100 bar reported in Table 3). Analyzing Fig. 4b, a pore cell density of 4.1E6 cells/cm^3, a void fraction of 0.84, an average pore size of 56 ± 28 μm, and an isotropy factor of 77 % were detected.

The images reported in Fig. 4c and Fig. 4d correspond to a sample processed under the same operating conditions but containing 10 g/g polymer-to-*karkadé* ratio. Also in this case, a uniform porous structure was achieved, with an average density of 200 ± 20 kg/m^3. Analyzing Fig. 4c, a cell density of 4.2E5 cells/cm^3, a void fraction of 0.83, an average pore diameter of 97 ± 63 μm, and an isotropy factor of 89 % were detected.

Having similar densities, void fraction was not significantly affected by the presence of *karkadé*. However, the presence of the bioactive induced polymer-drug interactions, thus inducing coalescence phenomena and an increase of cell size and sphericity, while decreasing the cell numerosity. As a final comment, the microporosity induced by gas expansion was characterized by a good degree of interconnection, as shown in both loaded and not loaded samples, constituting a unique porous network interconnected by quite uniform distribution.

5.2.4. Release kinetics

Release profiles obtained from foams produced at 45 °C and 100 bar were compared, considering the effect of *karkadé* mass entrapped (Fig. 5a and Fig. 5b).

The effect of PCL-to-*karkadé* ratio on release rate has been reported in Fig. 5a. A lower content of *karkadé* in the processed foam resulted in a reduced cumulative release time of the extract. The release kinetic obtained for a ratio of 30 g/g reached its *plateau* after around 250 min, while the 10 g/g loaded sample after 600 min, while the most concentrated foam ended release after 750 min. While the initial burst may be similar for three cases (drug adsorbed on external cells interconnections), a larger release time is needed for most concentrated samples to desorb larger amount of *karkadé*.

The comparison of release kinetics from homogenous and not uniform loaded foams was shown in Fig. 5b. In order to perform this comparison, the amount of extract entrapped in these three samples was set at 0.30 g. Pore structure obtained with a sorption time of 30 min offered a more compact barrier to *karkadé* diffusion to the external aqueous bulk, than homogenous samples. Indeed, plateau was reached after over 1200 min. Instead, the sample prepared with 60 min sorption time resulted in a uniform pore creation, offering a less compact barrier to diffusion than not homogenous sample, thus resulting into a plateau of about 600 min. Similarly, the sample prepared with 90 min sorption time ended release of *karkadé* in about 620 min, thus confirming an almost overlapping behavior and a similar pore uniform structure. The behavior of not homogenous foam (30 min sorption time) could be considered as an additional resistance to diffusion, thus resulting in delayed *karkadé* release. This controlled release system could be linked to sorption time and being considered a process parameter to avoid side effects or unpleasant accumulation above toxic levels. In general, this tunability could be intended as an advantage in release kinetics, thus regulating the amount of molecule absorbed by cells.

Samples reported in Fig. 5b were also employed to measure the inhibition of the antioxidant power. In particular, the receiving aqueous

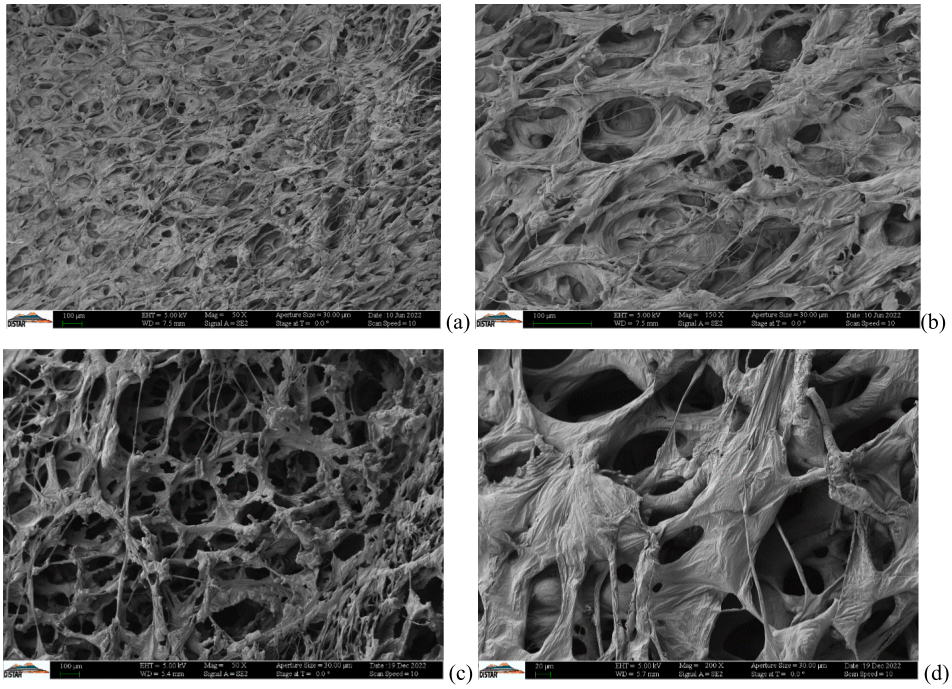

Fig. 4. SEM of unloaded PCL foam produced at 45 °C and 100 bar and 60 min with a magnitude of 50 × (a) and 150 × (b); PCL foam loaded with theoretical karkadé extract of 0.30 g, at the magnitude of 50 × (c) and 200 × (d).

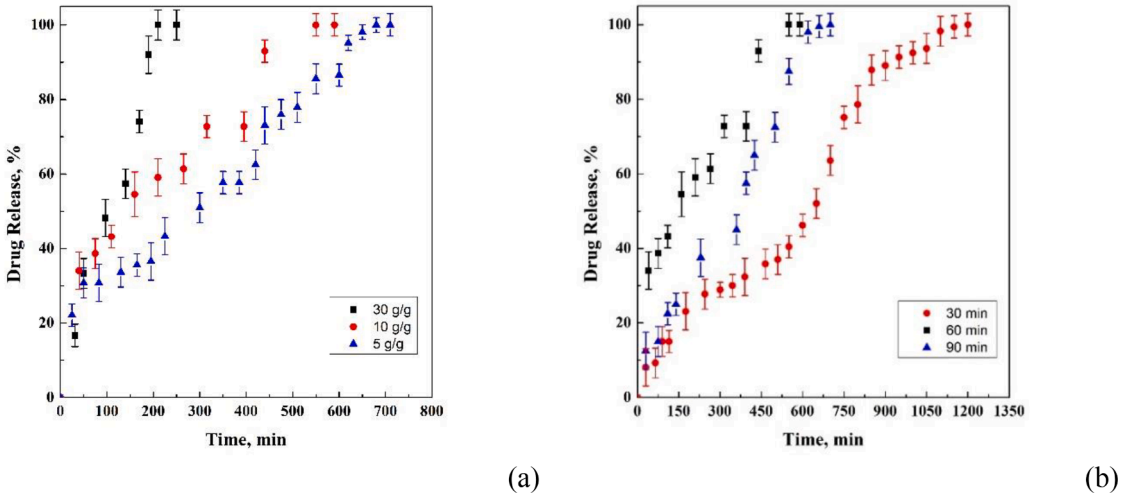

Fig. 5. PCL foams release tests evaluating polymer-to-drug ratio (a) and foaming sorption time (b) effects.

medium was withdrawn after the end of *karkadé* release and analyzed using the DPPH method, as described above. In particular, the samples produced with 30 min sorption resulted into inhibition of 32 %, while the other two were characterized by 28 and 31 %. This could be ascribed to the fact that saturated polymer offers a more homogeneous barrier (thus protection) to *karkadé* extract. This demonstrated that neither the foaming process affected significantly the antioxidant power of *karkadé*.

5.2.5. *Production of a patch-like prototype*

Following the results previously presented, the design of a first prototype of a commercial-like PCL patch has been attempted, with the aim of assessing the scalability of the high-pressure foaming process. While previous experiments were performed using a cubic aluminum mould, the creation of a patch-like foamed sample was supported by a rectangular geometry (95 × 12 × 10 mm^3). As it is possible to see in Fig. 6a, a sample with a larger volume at the center and lower volume at the two sides was produced. Temperature was set at 45 °C, pressure at 100 bar, and sorption time at 60 min. Properties of unloaded and *karkadé*-loaded foams were compared. Entrapment condition (30 g/g polymer-to-drug ratio) was chosen according to the highest EE obtained in previous experiments.

Concerning the unloaded sample, a density of 230 ± 40 kg/m^3 was achieved in the center of the patch-like sample, while a density of 350 ± 30 kg/m^3 was achieved at the samples extremities, due to the different free volume zones available for free expansion of PCL. Loaded sample replicated the same trend of the unloaded one. Since *karkadé* EE was higher in the sides (91.5 %) and equal to 81.3 % in the center, it could be affirmed that there is a competing different release rate of *karkadé* among the sides and the center, thus contributing to the tunability of the

Table 5
Patch-like unloaded and loaded foams.

Mould geometry	Zone	Foam density, kg/m^3	EE foam, %	ER, %
unloaded	side	350 ± 30	–	325
	core	230 ± 40	–	505
loaded	side	320 ± 20	91.5	358
	core	260 ± 20	81.3	445

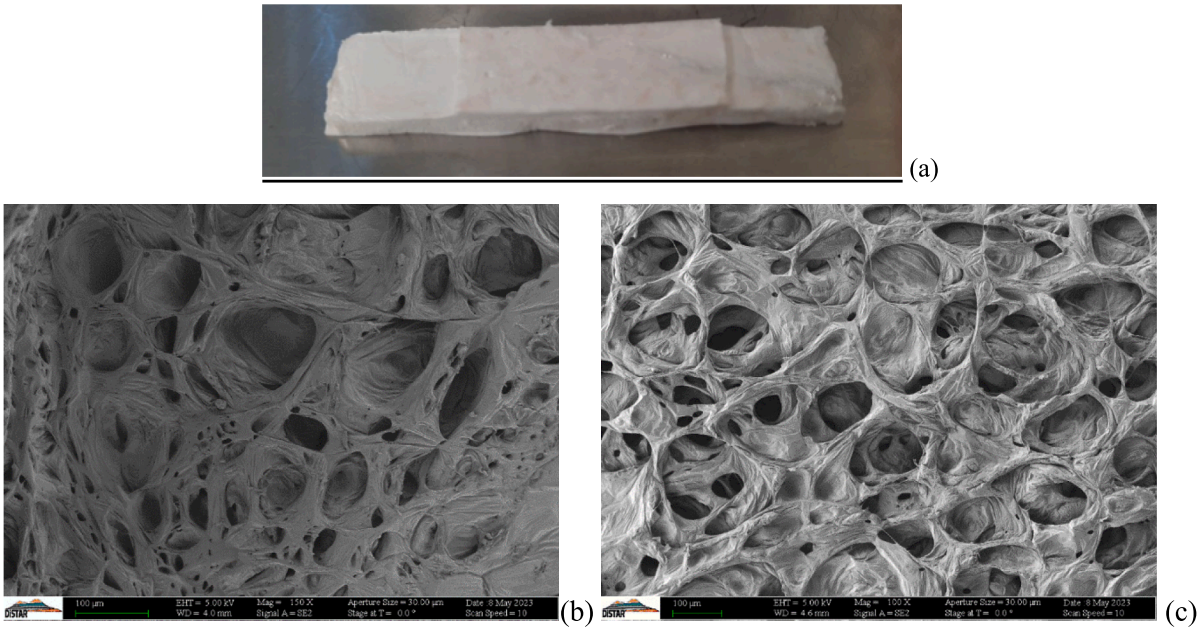

Fig. 6. Patch-like foamed sample: macroscopic (a) and SEM observations at the extremities (b) and in the center (c).

patch-like sample (Table 5). Fig. 6 reports representative photograph and microphotographs of the extremity (Fig. 6b) and of the center (Fig. 6c) of patch-like samples.

Fig. 6b represents one of the two sides of the patch-like prototype; as it is possible to see, it has a different structure than Fig. 6c. This last, being taken from the observation of the sample center, appears more uniform than the sides, also considering its lower cell number density (7.7E05 cell/cm^3) and larger pore diameter (64 ± 47 μm). Concerning the sides, Fig. 6b revealed a wider distribution of pores (cell number density of 3.6E06 cell/cm^3 and pores dimensions of 35 ± 32 μm). Cell density in the center had similar order of magnitude of the loaded sample reported in Fig. 4c. Smaller pores and larger cell density found in the sides are due to the different mass distribution among sample areas. This difference in pores distribution could be furthermore improved to adapt this patch to human skin.

5.2.6. Cell viability

In recent years, there has been a growing interest in developing materials that not only serve their intended purposes efficiently but also interact harmoniously with biological systems. Biocompatibility, a crucial aspect in medical and biological applications, ensures that materials do not elicit adverse reactions when in contact with living tissues. In this study, we investigate the biocompatibility of the produced foams, aiming to assess their suitability for biomedical applications. To achieve this goal, human keratinocyte cells (HaCaT) have been used. The cell viability was registered, over a total period of 9 days by MTS assay, culturing cells in CM obtained soaking the foams in DMEM. As indicated in Fig. 7, the control was represented by cells grown in the absence of foams.

As shown in Fig. 7, the presence of foams in CM did not interfere with cellular vitality and growth. The bioactive molecules, released after 20 h of soaking, reached concentrations highly compatible with keratinocytes. *In vitro* studies revealed high cell viability and proliferation, indicating excellent cytocompatibility. The observed biocompatibility of the studied foams suggests their promising potential for various biomedical applications. Their ability to support cell growth and tissue integration without eliciting adverse reactions signifies their suitability for tissue engineering, wound healing, and implantable medical devices. Furthermore, the versatility in foam composition and properties offers opportunities for tailored applications in specific biomedical contexts [74].

6. Conclusions

The primary objective of this study was to investigate optimal operating parameters to produce PCL foams through high pressure physical foaming. The project was addressed at the development of a biocompatible and lightweight foam for the controlled release of naturally occurring therapeutic extracts. After successfully reproducing and validating the results found in the literature, *karkadé*-loaded samples were produced, with a significant preservation of their AA despite the exposure to the foaming agent at high pressure conditions. The study examined polymer-to-drug ratio on release kinetics, revealing a consistent trend: lower extract content corresponded to shorter release times. Furthermore, comparing release kinetics between uniform and not uniform foams showed that sorption time affected pore distribution, cell density and dimensions. Shorter sorption times resulted in denser barriers to *karkadé* diffusion, leading to prolonged release durations. Conversely, longer sorption times yielded more uniform pore structures and less dense barriers, resulting in shorter *karkadé* release durations. This release system, regulated by sorption time, represents a significant achievement for fine-tuning drug delivery to mitigate adverse effects or toxicity and providing precise control over molecule uptake by cells. Indeed, the patch-like samples have been demonstrated to be biocompatible with skin cells, opening to a range of potential applications in the cosmetic and pharmaceutical fields.

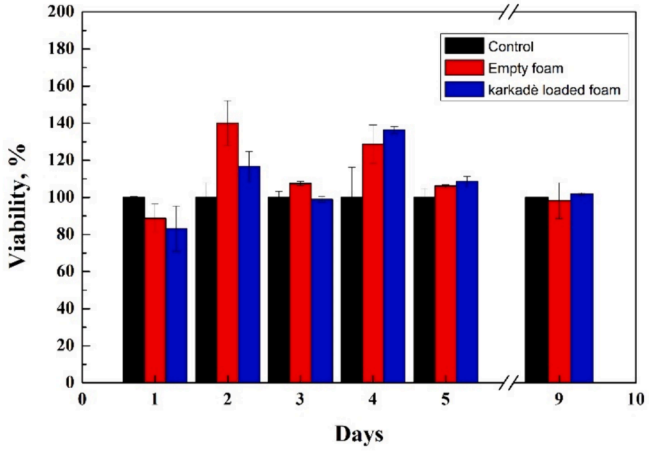

Fig. 7. Cell viability test performed on empty (red) and *karkadé*-loaded foams (blue) at 9 days of contact with human keratinocytes.

CRediT authorship contribution statement

Paolo Trucillo: Writing – review & editing, Writing – original draft, Visualization, Validation, Supervision, Resources, Project administration, Methodology, Investigation, Formal analysis, Data curation, Conceptualization. **Viviana Nebbioso:** Visualization, Validation, Methodology, Formal analysis, Data curation. **Pier Francesco Ferrari:** Visualization, Validation, Formal analysis, Data curation, Conceptualization. **Daniele Naviglio:** Validation, Methodology, Formal analysis, Data curation, Conceptualization. **Ernesto Di Maio:** Writing – review & editing, Validation, Resources, Methodology, Investigation, Formal analysis, Data curation, Conceptualization.

Declaration of competing interest

The authors declare that they have no known competing financial interests or personal relationships that could have appeared to influence the work reported in this paper.

Data availability

Data will be made available on request.

Appendix A. Supplementary material

Supplementary data to this article can be found online at https://doi.org/10.1016/j.eurpolymj.2024.113308.

References

[1] G. Riaz, R. Chopra, A review on phytochemistry and therapeutic uses of Hibiscus sabdariffa L, Biomed. Pharmacother. 102 (2018), https://doi.org/10.1016/j.biopha.2018.03.023.
[2] M.P. Sobantu, B.I. Okeleye, V.I. Okudoh, M. Meyer, Y.G. Aboua, In vitro antioxidant mechanism of action of Hibiscus Sabdariffa in the induction of apoptosis against breast cancer, J. Herbs Spices Med. Plants 29 (2023), https://doi.org/10.1080/10496475.2022.2135661.
[3] C.N. Chukwu, C.U. Ogunka-Nnoka, J.O. Akaninwor, Phytochemical composition, anti-nutrient properties and antioxidant potentials of raw Hibiscus sabdariffa seeds, Arch. Curr. Res. Int. 17 (2019), https://doi.org/10.9734/acri/2019/v17i330113.
[4] Y.B. Laskar, P.B. Mazumder, Insight into the molecular evidence supporting the remarkable chemotherapeutic potential of Hibiscus sabdariffa L, Biomed. Pharmacother. 127 (2020), https://doi.org/10.1016/j.biopha.2020.110153.
[5] H.E. Tahir, Z. Xiaobo, A.A. Mariod, G.K. Mahunu, M.A.Y. Abdualrahman, W. Tchabo, Assessment of antioxidant properties, instrumental and sensory aroma profile of red and white Karkade/Roselle (Hibiscus sabdariffa L.), J. Food Meas. Charact. 11 (2017), https://doi.org/10.1007/s11694-017-9535-0.

[6] H.O. Agunbiade, T.N. Fagbemi, T.A. Aderinola, Antioxidant properties of beverages from graded mixture of green/roasted coffee and hibiscus sabdariffa calyx flours, Appl. Food Res. 2 (2022), https://doi.org/10.1016/j.afres.2022.100163.
[7] A.M. Kazi, R. Dva, Characterization of continuous Hibiscus sabdariffa fibre reinforced epoxy composites, Polymers and Polymer Composites 30 (2022) 09673911211060957, https://doi.org/10.1177/09673911211060957.
[8] Q. Fitrotunnisa, A. Arsianti, N.A. Tejaputri, F. Qorina, Antioxidative activity and phytochemistry profile of hibiscus sabdariffa herb extracts, Int. J. Appl. Pharma. 11 (2019), https://doi.org/10.22159/ijap.2019.v11s6.33532.
[9] Q. Fithrotunnisa, A. Arsianti, G. Kurniawan, F. Qorina, N.A. Tejaputri, N.N. Azizah, In vitro cytotoxicity of Hibiscus sabdariffa Linn extracts on A549 lung cancer cell line, Pharmacogn. J. 12 (2020), https://doi.org/10.5530/pj.2020.12.3.
[10] R. Kamyab, H. Namdar, M. Torbati, M. Araj-Khodaei, M. Ghojazadeh, S.M. B. Fazljou, Pharmaceutical properties of Hibiscus sabdariffa, toward an ideal treatment for hypertension, Pharma. Sci. 28 (2022), https://doi.org/10.34172/PS.2021.68.
[11] J.A. Izquierdo-Vega, D.A. Arteaga-Badillo, M. Sánchez-Gutiérrez, J.A. Morales-González, N. Vargas-Mendoza, C.A. Gómez-Aldapa, J. Castro-Rosas, L. Delgado-Olivares, E. Madrigal-Bujaidar, E. Madrigal-Santillán, Organic acids from Roselle (Hibiscus sabdariffa L.)-A brief review of its pharmacological effects, Biomedicines 8 (2020), https://doi.org/10.3390/BIOMEDICINES8050100.
[12] N. Kamaly, Z. Xiao, P.M. Valencia, A.F. Radovic-Moreno, O.C. Farokhzad, Targeted polymeric therapeutic nanoparticles: Design, development and clinical translation, Chem. Soc. Rev. 41 (2012), https://doi.org/10.1039/c2cs15344k.
[13] Y. Zhang, T. Jiang, Q. Zhang, S. Wang, Inclusion of telmisartan in mesocellular foam nanoparticles: Drug loading and release property, Eur. J. Pharm. Biopharm. 76 (2010), https://doi.org/10.1016/j.ejpb.2010.05.010.
[14] J. Majumder, T. Minko, Multifunctional and stimuli-responsive nanocarriers for targeted therapeutic delivery, Expert Opin. Drug Deliv. 18 (2021), https://doi.org/10.1080/17425247.2021.1828339.
[15] M.X.L. Tan, M.K. Danquah, Drug and protein encapsulation by emulsification: Technology enhancement using foam formulations, Chem. Eng. Technol. 35 (2012), https://doi.org/10.1002/ceat.201100358.
[16] M.Y. Kim, J. Kim, Chitosan microgels embedded with catalase nanozyme-loaded mesocellular silica foam for glucose-responsive drug delivery, ACS Biomater. Sci. Eng. 3 (2017), https://doi.org/10.1021/acsbiomaterials.6b00716.
[17] P. Trucillo, E. Di Maio, Classification and production of polymeric foams among the systems for wound treatment, Polymers (Basel) 13 (2021), https://doi.org/10.3390/polym13101608.
[18] A.B. Hegge, T. Andersen, J.E. Melvik, E. Bruzell, S. Kristensen, H.H. Tønnesen, Formulation and bacterial phototoxicity of curcumin loaded alginate foams for wound treatment applications: Studies on curcumin and curcuminoides XLII, J. Pharm. Sci. 100 (2011), https://doi.org/10.1002/jps.22263.
[19] S. Gao, S. Chen, S. Li, Z. Ye, L. Deng, A. Dong, Preparation and characterization of dual-antibiotic-loaded hydrophilic polyurethane foam, Chem. Industry Eng. 39 (2022), https://doi.org/10.13353/j.issn.1004.9533.20210106.
[20] C. Canal, R.M. Aparicio, A. Vílchez, J. Esquena, M.J. García-Celma, Drug delivery properties of macroporous polystyrene solid foams, J. Pharm. Pharm. Sci. 15 (2012), https://doi.org/10.18433/j3x884.
[21] K.A. Kravanja, M. Finšgar, Ž. Knez, M. Knez Marevci, Supercritical fluid technologies for the incorporation of synthetic and natural active compounds into materials for drug formulation and delivery, Pharmaceutics 14 (2022), https://doi.org/10.3390/pharmaceutics14081670.
[22] A. Rai, S. Senapati, S.K. Saraf, P. Maiti, Biodegradable poly(ϵ-caprolactone) as a controlled drug delivery vehicle of vancomycin for the treatment of MRSA infection, J. Mater. Chem. B 4 (2016), https://doi.org/10.1039/c6tb01623e.
[23] T.K. Dash, V.B. Konkimalla, Poly-ε-caprolactone based formulations for drug delivery and tissue engineering: A review, J. Control. Release 158 (2012), https://doi.org/10.1016/j.jconrel.2011.09.064.
[24] N.K. Singh, S.K. Singh, D. Dash, B.P. Das Purkayastha, J.K. Roy, P. Maiti, Nanostructure controlled anti-cancer drug delivery using poly(ε-caprolactone) based nanohybrids, J. Mater. Chem. 22 (2012), https://doi.org/10.1039/c2jm32340k.
[25] Š. Zupančič, L. Preem, J. Kristl, M. Putrinš, T. Tenson, P. Kocbek, K. Kogermann, Impact of PCL nanofiber mat structural properties on hydrophilic drug release and antibacterial activity on periodontal pathogens, Eur. J. Pharm. Sci. 122 (2018), https://doi.org/10.1016/j.ejps.2018.07.024.
[26] B. Rai, S.H. Teoh, D.W. Hutmacher, T. Cao, K.H. Ho, Novel PCL-based honeycomb scaffolds as drug delivery systems for rhBMP-2, Biomaterials 26 (2005), https://doi.org/10.1016/j.biomaterials.2004.09.052.
[27] Z. Yang, T. Liu, D. Hu, Z. Xu, L. Zhao, Foaming window for preparation of microcellular rigid polyurethanes using supercritical carbon dioxide as blowing agent, J. Supercrit. Fluids 147 (2019), https://doi.org/10.1016/j.supflu.2018.11.001.
[28] H.Y. Mi, X. Jing, J. Peng, M.R. Salick, X.F. Peng, L.S. Turng, Poly(ε-caprolactone) (PCL)/cellulose nano-crystal (CNC) nanocomposites and foams, Cellul. 21 (2014), https://doi.org/10.1007/s10570-014-0327-y.
[29] S. Milovanovic, D. Markovic, A. Mrakovic, R. Kuska, I. Zizovic, S. Frerich, J. Ivanovic, Supercritical CO2 - assisted production of PLA and PLGA foams for controlled thymol release, Mater. Sci. Eng. C 99 (2019), https://doi.org/10.1016/j.msec.2019.01.106.
[30] L. Lu, S.J. Peter, M.D. Lyman, H.L. Lai, S.M. Leite, J.A. Tamada, S. Uyama, J. P. Vacanti, R. Langer, A.G. Mikos, In vitro and in vivo degradation of porous poly (DL-lactic-co-glycolic acid) foams, Biomaterials 21 (18) (2000) 1837–1845, https://doi.org/10.1016/S0142-9612(00)00047-8.
[31] B.Y.S. Ong, S.H. Ranganath, L.Y. Lee, F. Lu, H.S. Lee, N.V. Sahinidis, C.H. Wang, Paclitaxel delivery from PLGA foams for controlled release in post-surgical chemotherapy against glioblastoma multiforme, Biomaterials 30 (2009), https://doi.org/10.1016/j.biomaterials.2009.02.030.
[32] Y. Savelyev, V. Veselov, L. Markovskaya, O. Savelyeva, E. Akhranovich, N. Galatenko, L. Robota, T. Travinskaya, Preparation and characterization of new biologically active polyurethane foams, Mater. Sci. Eng. C 45 (2014), https://doi.org/10.1016/j.msec.2014.08.068.
[33] A. Testouri, C. Honorez, A. Barillec, D. Langevin, W. Drenckhan, Highly structured foams from chitosan gels, Macromolecules 43 (2010), https://doi.org/10.1021/ma100819j.
[34] A. Piotrowska-Kirschling, A. Olszewski, J. Karczewski, Ł. Piszczyk, J. Brzeska, Synthesis and physicochemical characteristics of chitosan-based polyurethane flexible foams, Processes 9 (2021), https://doi.org/10.3390/pr9081394.
[35] F. Guo, W. Zhang, X. Pei, X. Shen, Q. Yan, W. Hong, G. Yang, Synthesis, characterization, and cytotoxicity of star-shaped polyester-based elastomers as controlled release systems for proteins, J. Appl. Polym. Sci. 133 (2016), https://doi.org/10.1002/app.43393.
[36] J.N. Hoskins, S.M. Grayson, Synthesis and degradation behavior of cyclic poly (ε-caprolactone), Macromolecules 42 (2009), https://doi.org/10.1021/ma9011076.
[37] M.J. Jenkins, K.L. Harrison, M.M.C.G. Silva, M.J. Whitaker, K.M. Shakesheff, S. M. Howdle, Characterisation of microcellular foams produced from semi-crystalline PCL using supercritical carbon dioxide, Eur. Polym. J. 42 (2006), https://doi.org/10.1016/j.eurpolymj.2006.07.022.
[38] V.R. Sinha, K. Bansal, R. Kaushik, R. Kumria, A. Trehan, Poly-ε-caprolactone microspheres and nanospheres: An overview, Int. J. Pharm. 278 (2004), https://doi.org/10.1016/j.ijpharm.2004.01.044.
[39] M. Ansari, S. Salahshour-Kordestani, M. Habibi-Rezaei, A.A.M. Movahedi, Synthesis and characterization of acylated polycaprolactone (PCL) nanospheres and investigation of their influence on aggregation of amyloid proteins, J. Macromol. Sci. Part B: Phys. 54 (2015), https://doi.org/10.1080/00222348.2014.984578.
[40] N. Raina, R. Pahwa, J.K. Khosla, P.N. Gupta, M. Gupta, Polycaprolactone-based materials in wound healing applications, Polym. Bull. 79 (2022), https://doi.org/10.1007/s00289-021-03865-w.
[41] E. Malikmammadov, T.E. Tanir, A. Kiziltay, V. Hasirci, N. Hasirci, PCL and PCL-based materials in biomedical applications, J. Biomater. Sci. Polym. Ed. 29 (2018), https://doi.org/10.1080/09205063.2017.1394711.
[42] E. Archer, M. Torretti, S. Madbouly, Biodegradable polycaprolactone (PCL) based polymer and composites, Phys. Sci. Rev. 8 (2023), https://doi.org/10.1515/psr-2020-0074.
[43] M.R. Dethe, A. Prabakaran, H. Ahmed, M. Agrawal, U. Roy, A. Alexander, PCL-PEG copolymer based injectable thermosensitive hydrogels, Journal of Controlled Release 343 (2022) 217–236, https://doi.org/10.1016/j.jconrel.2022.01.035.
[44] E.J. Chong, T.T. Phan, I.J. Lim, Y.Z. Zhang, B.H. Bay, S. Ramakrishna, C.T. Lim, Evaluation of electrospun PCL/gelatin nanofibrous scaffold for wound healing and layered dermal reconstitution, Acta Biomater. 3 (2007), https://doi.org/10.1016/j.actbio.2007.01.002.
[45] M. Abrisham, M. Noroozi, M. Panahi-Sarmad, M. Arjmand, V. Goodarzi, Y. Shakeri, H. Golbaten-Mofrad, P. Dehghan, A. Seyfi Sahzabi, M. Sadri, L. Uzun, The role of polycaprolactone-triol (PCL-T) in biomedical applications: A state-of-the-art review, Eur. Polym. J. 131 (2020), https://doi.org/10.1016/j.eurpolymj.2020.109701.
[46] J.H. Lee, J.K. Park, K.H. Son, J.W. Lee, PCL/sodium-alginate based 3D-printed dual drug delivery system with antibacterial activity for osteomyelitis therapy, Gels 8 (2022), https://doi.org/10.3390/gels8030163.
[47] L. Marincaș, N.I. Farkas, L. Barbu-Tudoran, R. Barabás, M.I. Toșa, Deep eutectic solvent PCL-based nanofibers as drug delivery system, Mater. Chem. Phys. 304 (2023), https://doi.org/10.1016/j.matchemphys.2023.127862.
[48] P. Grossen, D. Witzigmann, S. Sieber, J. Huwyler, PEG-PCL-based nanomedicines: A biodegradable drug delivery system and its application, J. Control. Release 260 (2017), https://doi.org/10.1016/j.jconrel.2017.05.028.
[49] M. Karimi, M. Heuchel, T. Weigel, M. Schossig, D. Hofmann, A. Lendlein, Formation and size distribution of pores in poly(ε-caprolactone) foams prepared by pressure quenching using supercritical CO 2, J. Supercrit. Fluids 61 (2012), https://doi.org/10.1016/j.supflu.2011.09.022.
[50] O.C. Onder, E. Yilgor, I. Yilgor, Preparation of monolithic polycaprolactone foams with controlled morphology, Polymer (Guildf) 136 (2018), https://doi.org/10.1016/j.polymer.2017.12.054.
[51] S. Ahadian, J.A. Finbloom, M. Mofidfar, S.E. Diltemiz, F. Nasrollahi, E. Davoodi, V. Hosseini, I. Mylonaki, S. Sangabathuni, H. Montazerian, K. Fetah, R. Nasiri, M. R. Dokmeci, M.M. Stevens, T.A. Desai, A. Khademhosseini, Micro and nanoscale technologies in oral drug delivery, Adv. Drug Deliv. Rev. 157 (2020), https://doi.org/10.1016/j.addr.2020.07.012.
[52] Y. Wang, G. Chen, H. Zhang, C. Zhao, L. Sun, Y. Zhao, Emerging functional biomaterials as medical patches, ACS Nano 15 (2021), https://doi.org/10.1021/acsnano.0c10724.
[53] J. He, Y. Zhang, X. Yu, C. Xu, Wearable patches for transdermal drug delivery, Acta Pharm. Sin. B 13 (2023), https://doi.org/10.1016/j.apsb.2023.05.009.
[54] L.F. Santos, I.J. Correia, A.S. Silva, J.F. Mano, Biomaterials for drug delivery patches, Eur. J. Pharm. Sci. 118 (2018), https://doi.org/10.1016/j.ejps.2018.03.020.
[55] M. Gallo, A. Formato, M. Ciaravolo, G. Formato, D. Naviglio, Study of the kinetics of extraction process for the production of hemp inflorescences extracts by means

of conventional maceration (CM) and rapid solid-liquid dynamic extraction (RSLDE), Separations 7 (2020), https://doi.org/10.3390/separations7020020.
[56] Q. Xu, X. Ren, Y. Chang, J. Wang, L. Yu, K. Dean, Generation of microcellular biodegradable polycaprolactone foams in supercritical carbon dioxide, J. Appl. Polym. Sci. 94 (2004), https://doi.org/10.1002/app.20726.
[57] D. Naviglio, P. Scarano, M. Ciaravolo, M. Gallo, Rapid solid-liquid dynamic extraction (RSLDE): A powerful and greener alternative to the latest solid-liquid extraction techniques, Foods 8 (2019), https://doi.org/10.3390/foods8070245.
[58] D. Naviglio, D. Montesano, M. Gallo, Laboratory production of lemon liqueur (Limoncello) by conventional maceration and a two-syringe system to illustrate rapid solid-liquid dynamic extraction, J. Chem. Educ. 92 (2015), https://doi.org/10.1021/ed400379g.
[59] E. Di Maio, G. Mensitieri, S. Iannace, L. Nicolais, W. Li, R.W. Flumerfelt, Structure optimization of polycaprolactone foams by using mixtures of CO 2 and N 2 as blowing agents, Polym. Eng. Sci. 45 (2005), https://doi.org/10.1002/pen.20289.
[60] C. Marrazzo, E. Di Maio, S. Iannace, L. Nicolais, Process-structure relationships in PCL foaming, J. Cell. Plast. 44 (2008), https://doi.org/10.1177/0021955X07079147.
[61] S. Baliyan, R. Mukherjee, A. Priyadarshini, A. Vibhuti, A. Gupta, R.P. Pandey, C. M. Chang, Determination of antioxidants by DPPH radical scavenging activity and quantitative phytochemical analysis of Ficus religiosa, Molecules 27 (2022), https://doi.org/10.3390/molecules27041326.
[62] C. Marrazzo, E. Di Maio, S. Iannace, Conventional and nanometric nucleating agents in poly(ε-caprolactone) foaming: Crystals vs. bubbles nucleation, Polym. Eng. Sci. 48 (2008), https://doi.org/10.1002/pen.20937.
[63] V. Guarino, F. Causa, L. Ambrosio, Porosity and mechanical properties relationship in PCL porous scaffolds, J. Appl. Biomater. Biomech. 5 (2007), https://doi.org/10.1177/228080000700500303.
[64] R. Mohamed, J. Fernández, M. Pineda, M. Aguilar, Roselle (Hibiscus sabdariffa) seed oil is a rich source of γ-tocopherol, J. Food Sci. 72 (2007), https://doi.org/10.1111/j.1750-3841.2007.00285.x.
[65] R.S. Kalhapure, C. Mocktar, D.R. Sikwal, S.J. Sonawane, M.K. Kathiravan, A. Skelton, T. Govender, Ion pairing with linoleic acid simultaneously enhances encapsulation efficiency and antibacterial activity of vancomycin in solid lipid nanoparticles, Colloids Surf. B Biointerfaces 117 (2014), https://doi.org/10.1016/j.colsurfb.2014.02.045.
[66] W. Khuntawee, R. Amornloetwattana, W. Vongsangnak, K. Namdee, T. Yata, M. Karttunen, J. Wong-Ekkabut, In silicoandin vitrodesign of cordycepin encapsulation in liposomes for colon cancer treatment, RSC Adv. 11 (2021), https://doi.org/10.1039/d1ra00038a.
[67] G. Baysal, H.S. Olcay, B. Keresteci, H. Özpinar, The antioxidant and antibacterial properties of chitosan encapsulated with the bee pollen and the apple cider vinegar, J. Biomater. Sci. Polym. Ed. 33 (2022), https://doi.org/10.1080/09205063.2022.2031463.
[68] L. Baldino, S. Cardea, Generation of biocompatible PCL foams by supercritical foaming, Chem. Eng. Trans. 79 (2020), https://doi.org/10.3303/CET2079041.
[69] D. Knani, D. Alperstein, T. Kauth, D. Kaltbeitzel, C. Hopmann, Molecular modeling study of CO2 plasticization and sorption onto absorbable polyesters, Polym. Bull. 72 (2015), https://doi.org/10.1007/s00289-015-1349-9.
[70] C.X. Chen, Q.Q. Liu, X. Xin, Y.X. Guan, S.J. Yao, Pore formation of poly (ε-caprolactone) scaffolds with melting point reduction in supercritical CO2 foaming, J. Supercrit. Fluids 117 (2016), https://doi.org/10.1016/j.supflu.2016.07.006.
[71] I. Ushiki, H. Kawashima, S.I. Kihara, S. Takishima, Solubility and diffusivity of supercritical CO2 for polycaprolactone in its molten state: Measurement and modeling using PC-SAFT and free volume theory, The Journal of Supercritical Fluids 181 (2022) 105499, https://doi.org/10.1016/j.supflu.2021.105499.
[72] R. Campardelli, P. Franco, E. Reverchon, I. De Marco, Polycaprolactone/nimesulide patches obtained by a one-step supercritical foaming + impregnation process, J. Supercrit. Fluids 146 (2019), https://doi.org/10.1016/j.supflu.2019.01.008.
[73] M. Guastaferro, L. Baldino, S. Cardea, E. Reverchon, Supercritical processing of PCL and PCL-PEG blends to produce improved PCL-based porous scaffolds, J. Supercrit. Fluids 186 (2022), https://doi.org/10.1016/j.supflu.2022.105611.
[74] Y. Zhou, Y. Tian, M. Zhang, Technical development and application of supercritical CO2 foaming technology in PCL foam production, Sci. Rep. 14 (2024), https://doi.org/10.1038/s41598-024-57545-6.